03,09,12

Luminescent properties of colloidal Ag_2S quantum dots for photocatalytic applications

© O.V. Ovchinnikov, M.S. Smirnov, S.V. Aslanov¶, A.S. Perepelitsa

Voronezh State University,
Voronezh, Russia

¶ E-mail: Windmaster7@yandex.ru

Received July 8, 2021
Revised July 8, 2021
Accepted July 8, 2021

The structural and optical properties of colloidal Ag_2S quantum dots in various environments are investigated. With the help of transmission electron microscopy, X-ray diffraction and energy-dispersive X-ray analysis the formation of colloidal Ag_2S quantum dots with an average size of 2−3 nm with a monoclinic crystal lattice, and Ag_2S/SiO_2 core-shell systems based on them, has been established. The change in the luminescence quantum yield of quantum dots with the change of the surface environment state is shown. The decoration of TiO_2 nanoparticles of 10−15 nm in size with Ag_2S quantum dots was performed and the influence of the structure of the interfaces of quantum dots and their environment (2-mercaptopropionic acid, water, ethylene glycol, SiO_2 dielectric shell with a thickness of 0.6 nm and 2.0 nm) on the formation of TiO_2-Ag_2S heterosystems was analyzed. For Ag_2S quantum dots passivated with 2-mercaptopropionic acid, signs of charge phototransfer after adsorption on TiO_2 nanoparticles surface have been established. Signs of reactive oxygen species appearance due to charge phototransfer in heterosystem are enstablished, based on methylene blue photobleaching under excitation of heterosystem outside of TiO_2 fundamental absorption region,

Keywords: Quantum dots, photocatalysis, luminescence, titanium dioxide, silver sulfide.

DOI: 10.21883/PSS.2022.13.52302.19s

1. Introduction

Today, development of photocatalytic systems for various applications is of a high interest [1–5]. For their creation the most suitable material is Titanium Dioxide (TiO_2) [6–10]. Titanium Dioxide has unique photocatalytic properties, however, the fundamental absorption edge of photocatalyst active phases of Titanium Dioxide — rutile and anatase is within the spectral region shorter than 400 nm [11,12]. Therefore, there is a problem of the Titanium Dioxide sensitization to visible radiation. Colloidal quantum dots of narrow-band semiconductor compounds have suitable spectral properties controlled by the size effect [13–15]. A promising candidate for the role of efficient photo sensitizer is silver sulfide (Ag_2S). It is non-toxic, insoluble in water, and chemically stable. Ag_2S colloidal quantum dots (QDs) have size-dependent spectrum of optical absorption, which can be shifted from the near IR region to the edge of the visible range [16–20]. Decoration of TiO_2 surface by Ag_2S QD's can lead to increase in spectral sensitivity range of TiO_2 up to near infrared region [21]. In heterosystem TiO_2-Ag_2S, according to the literature data, in case of photo excitation Ag_2S QDs may serve as donors of electrons [22,23].

Optical properties of silver sulfide are generally determined by the method of manufacture and selected passivator [24–26]. Sizes of passivator molecules also matter for implementation of the charge carriers transfer processes. This is why there is a separate complicated problem of compatibility of the TiO_2-Ag_2S heterosystem components providing adsorption of QDs on the surface of TiO_2 and efficient charge phototransfer. Such heterosystems are able to produce reactive oxygen species (ROS), which is required for creation of photobactericide coatings and devices for water purification and disinfection [27].

Properties of hybrid nanosystems TiO_2-Ag_2S are incompletely covered in literature.

In this regard only certain studies are known [21–23,27,28]. Because of non-stoichiometry, significant contribution into photoprocesses in Ag_2S is provided by radiationless processes [29,30], which reduce both quantum yield of the QD luminescence, and the efficiency of sensitization of a photocatalyst. Therefore, selection of the conditions of synthesis of Ag_2S QDs with considerable quantum output of luminescence and the structure of interfaces ensuring efficient adsorption at nanocrystals TiO_2 is an actual task.

This work presents the results of study of structural and optical properties of colloidal Ag_2S QDs, passivated by 2-mercaptopropionic acid, as well as TiO_2 nanocrystals decorated with studied QDs. The presented results demonstrate signs of efficient production of reactive oxygen species when the system is exposed to the visible range light.

2. Studied samples

Studied samples of colloidal Ag_2S QDs were prepared by using the methodologies of colloidal synthesis realized with application of molecules of 2-mercaptopropionic acid

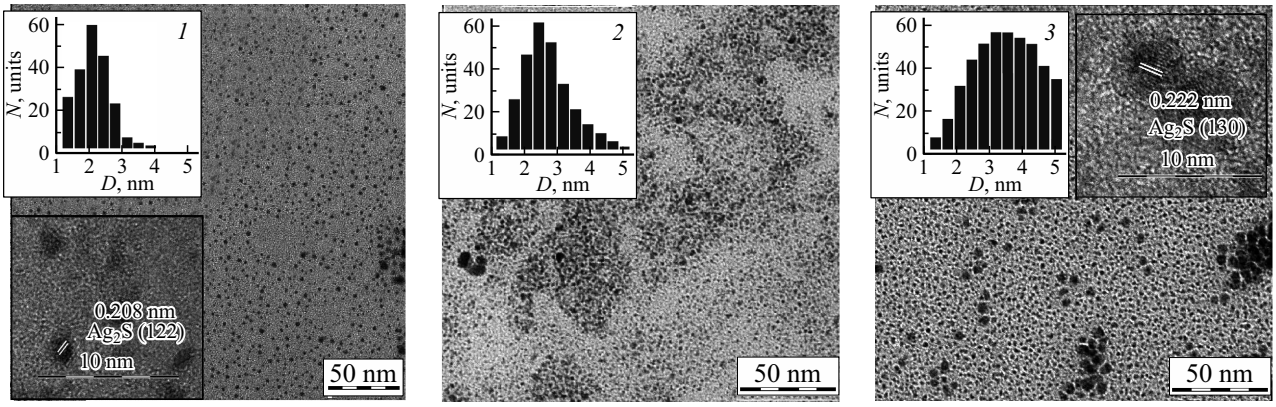

Figure 1. TEM-images and size distribution histograms of Ag_2S QDs samples: Ag_2S/2MPA/W — *1*, Ag_2S/MPTMS — *2*, Ag_2S/SiO_2 — *3*.

(2MPA) as a passivator in water medium, and in ethylene glycol.

Used reagents: silver nitrate ($AgNO_3$), 2-mercaptopropionic acid (2MPA), 3-mercaptopropyltrimethoxysilane (MPTMS), sodium metasilicate (Na_2SiO_3), ethylene glycol and sodium hydroxide (NaOH) by Sigma-Aldrich. The samples of photocatalyst of Titanium Dioxide IK-12-32 of the grade „A" were provided by Boreskov Institute of Catalysis SB RAS.

During synthesis of Ag_2S QDs in water (hereinafter referred to as Ag_2S/2MPA/W) as a precursor we used mixture 2MPA water solution with water solution of $AgNO_3$ with the ratio $[2MPA]:[AgNO_3] = 1:2$. After that, sulfur precursor was injected (Na_2S) with the ratio $[AgNO_3]:[2MPA]:[Na_2S] = 1:2:0.16$ [25].

Synthesis of QP Ag_2S in ethylene glycol (hereinafter referred to as Ag_2S/2MPA/EG) was performed according to the methodology described by us in [31].

For assembly of hybrid nanosystems [TiO_2-QP Ag_2S] nanocrytalline powder TiO_2 was dissolved in water and treated luminescence quantum yield ultrasound luminescence quantum yield the 60 kHz frequency until homogeneous suspension is formed. Then, the suspension was mixed with the solution of Ag_2S QDs and dried at room temperature. The produced dim-gray powder was washed to remove free QDs.

As reference samples featuring higher quantum yield of luminescence and low efficiency of injection of the charge carriers, we used SiO_2 dielectric-coated Ag_2S/SiO_2/2MPA QDs. The coating was formed by the method similar to that we applied in [30]. The use of MPTMS ensured the formation of monolayer SiO_2 shells (hereinafter referred to as Ag_2S/MPTMS QDs), and an increase in the shell thickness was achieved by using an aqueous solution of Na_2SiO_3 (hereinafter referred to as Ag_2S/SiO_2 QDs).

3. Methodologies of experimental studies

For measurement of optical absorption and luminescence spectra within the region of 200–1000 nm we used spectrophotometer USB-2000+XR1 (Ocean Optics, USA) with the radiation source USB-DT. For measurement of spectra of diffusion reflection spectrophotometer is additionally equipped with xenon lamp and integrating sphere. As the white standard we used barium sulfate applied to the substrate Al_2O_3.

For measurement of spectra of luminescence within the region of 800–1200 nm we used automatic spectrometer complex based on the diffraction monochromator MDR-4 (LOMO, Russia) using photo diode PDF-10C/M (ThorLabs, USA) as detector. Excitation sources were the LED module HPL-H77GV1BT-V1 (High Power Lighting Corp., Taiwan) with the wavelength of 365 nm and the laser module Osram LD PL-TB450 (Osram, Germany) with the wave length 445 nm.

Structural studies of source samples were performed by using the X-ray diffraction method by means of the diffractometer THERMO ARL X'TRA (ThermoFisher, Switzerland) and transmission electron microscopy by means of the microscope LIBRA 120 (CarlZeiss, Germany).

Measurement of luminescence quantum yield of the samples was performed by standard method of comparison with the reference [32], which was represented by the solution of indocyanine green in dymethyl sulfoxide with quantum yield of 13% [33].

4. Structural properties of the studied samples

Fig. 1 shows TEM images and size distribution histograms of the studied samples of Ag_2S QDs.

Original ensembles of Ag_2S/2MPA QDs consists of nanocrystals with the average size of 2.2 nm and size dispersion about 40%. Analysis of high-resolution TEM image shown diffraction of electrons from crystallographic plain (122) of monoclinic lattice of Ag_2S. Addition of 0.1 ppm of MPTMS resulted in increase of the average size of crystals to 2.6 nm with dispersion of about 35%. At the same time low-contrast phase formation is observed around crystals, which can be interpreted as weak scattering of

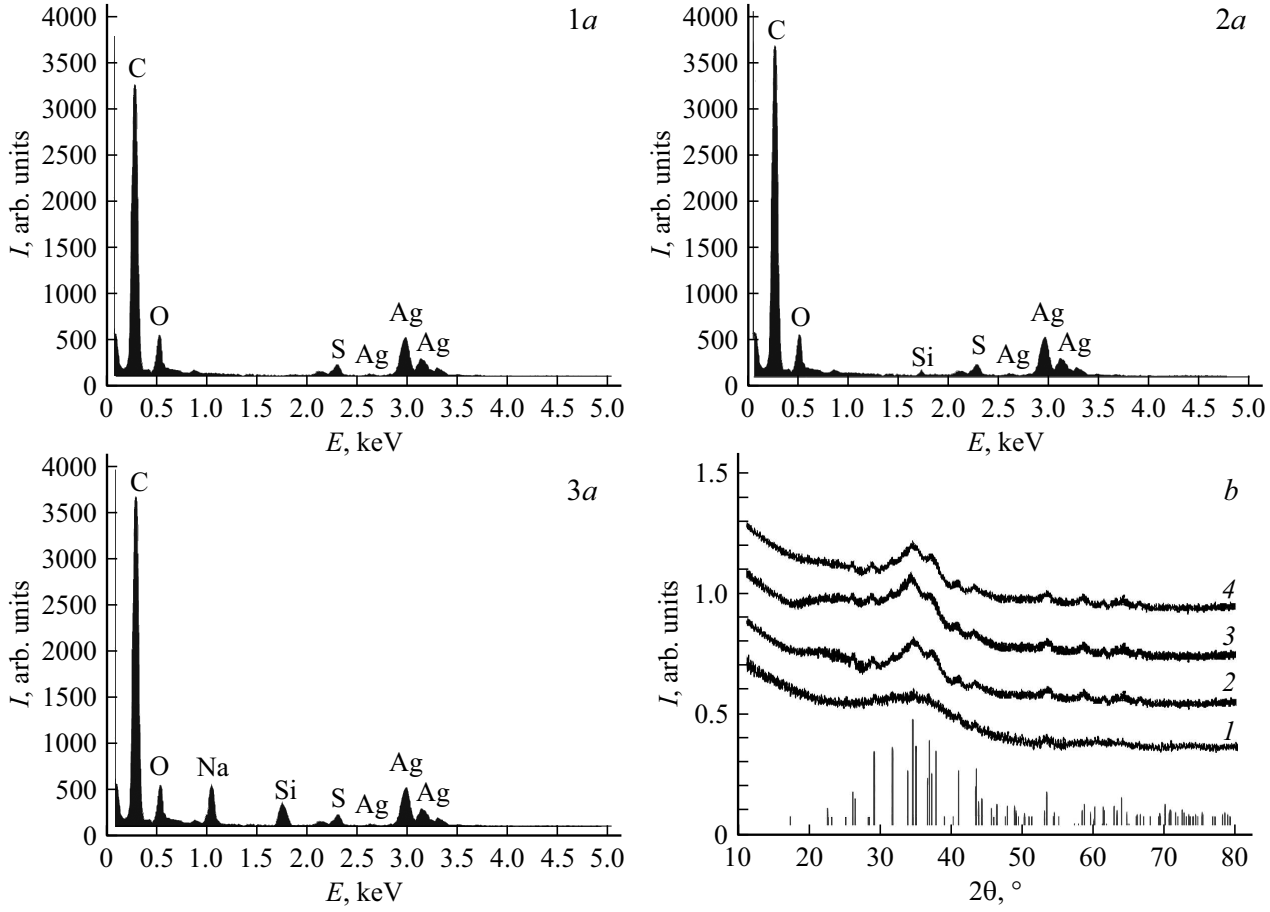

Figure 2. Spectra of EDX (*a*) and X-ray diffractograms (*b*) of the studied QD samples: Ag_2S/2MPA/W — *1*, Ag_2S/MPTMS — *2*, Ag_2S/SiO_2 — *3*, Ag_2S/2MPA/EG — *4*.

electrons on amorphous SiO_2 shell. After adding sodium metasilicate there was an increase in average size of QDs up to 3.5−4.0 nm with dispersion by size about 40% and formation of thicker shell around the samples. According to high-resolution TEM-image there is low-contrast shell with the thickness of 1 nm around the crystalline core of Ag_2S. Ag_2S/2MPA/EG QDs have average size about 2.4 nm with the size dispersion about 30%.

Results of EDX analysis of the QD samples are given in Fig. 2.

In case of Ag_2S/2MPA QDs there are emission lines of silver and sulfur atoms, as well as intensive peak of carbon atoms contained in the 2MPA molecules, as well as carbon substrate used during making the images. Presence of the lines of oxygen atoms is related to their presence in the 2MPA molecule. In case of the sample Ag_2S/MPTMS the spectrum shows a low peak in the region of 1.76 keV. It is related with the group of emission lines of the silicium atoms. This line is superposition of the lines $K_{\alpha 1}$ (1.739 keV), $K_{\alpha 2}$ (1.739 keV) and $K_{\beta 1}$ (1.835 keV). Also increase of intensity of the emission line $K_{\alpha 1}$ of oxygen (0.525 keV) is observed, which is the consequence of increase of the oxygen concentration during generation of SiO_2 shell.

Increase of intensity of the sulfur and carbon lines occurs due to their presence in the precursor MPTMS and, probably, it is a result of completion of growing of the crystalline nucleus of QDs. For the sample Ag_2S/SiO_2 intensity of the lines of silicium and oxygen increased, which is related with increase of the SiO_2 shell thickness, confirmed by the data of TEM. Also, in that sample there is a weak peak representing superposition of the lines of sodium $K_{\alpha 1}$ (1.05 keV) and $K_{\beta 1}$ (1.041 keV), associated with the use of precursor sodium metasilicate.

For confirmation of the crystalline structure Ag_2S QDs we obtained X-ray diffractograms for study of $K_{\alpha 1}$ copper (1.054 Å). For Ag_2S/2MPA/W QDs (Fig. 2, *b*, the curve *1*), Ag_2S/2MPA/EG QDs (Fig. 2, *b*, the curve *4*) in all cases on diffractograms there was a wide halo in the region 10−50°, caused by small sizes of studied crystallites. For Ag_2S/2MPA/EG QDs there were low intensive peaks on the halo background, whose position corresponds to that of the reflexes of monoclinic phase of Ag_2S (spatial group $P2_{1/c}$) [34]. Estimations of the medium size of crystallites made by using the Scherrer formula show the presence of crystallites with the average size of ~ 3 nm. In case of Ag_2S/2MPA/W QDs reflexes were not observed, which is caused by small size of crystallites.

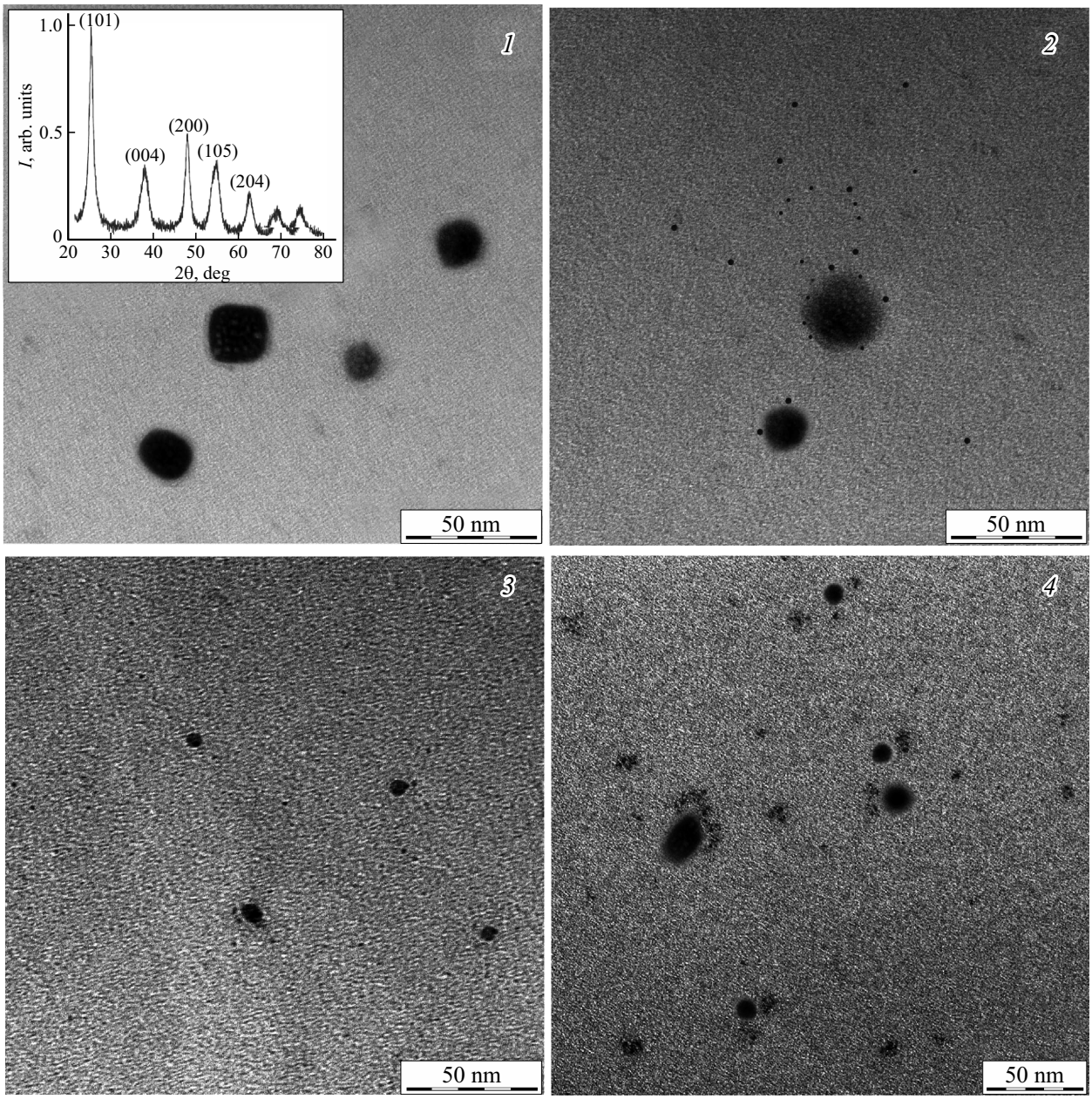

Figure 3. TEM-images of the studied samples: TiO_2 — *1*, TiO_2-Ag_2S/2MPA/W — *2*, TiO_2-Ag_2S/SiO_2 — *3*, TiO_2-Ag_2S/2MPA/EG — *4*. Inset includes X-ray diffractogram of the sample of nanoparticles TiO_2.

As a result of replacement of passivator for Ag_2S/2MPA/W QDs from 2-MPA to MPTMS (Fig. 2, *b*, the curve *2*) and further increase of the average size of crystallites there were reflexes on X-ray patterns, whose position corresponds to that of the reflexes of monoclinic phase of Ag_2S ($P2_{1/c}$). Formation of additional halo in the region of angles 15−25° is associated with formation of amorphous phase SiO_2 [35,36]. Further increase of the SiO_2 hell thickness with addition of the solution of sodium metasilicate (Fig. 1, *b*, the curve *3*) resulted in increase of halo intensity in the region 15−25°. Whereas the structure of reflexes associated with monoclinic phase of Ag_2S has not changed.

Fig. 3 shows TEM-images of nanoparticles TiO_2 and mixtures with Ag_2S QDs.

According to TEM, the samples of TiO_2 represent nanoparticles with the average size of 10−15 nm (Fig. 3, *1*). There is a series of clear peaks on the X-ray pattern, that correspond to the X-ray diffraction of crystalline TiO_2 in the anatase phase [37]. Estimation of sizes by using the Scherrer formula showed the average size of 11−13 nm, which correlates with the TEM results. TEM images showed congestion of Ag_2S and Ag_2S/SiO_2 QDs near TiO_2 nanoparticles surface.

Inversely thereto, in the mixture TiO_2-Ag_2S/2MPA/EG there was separation of QDs with nanoparticles. Probably,

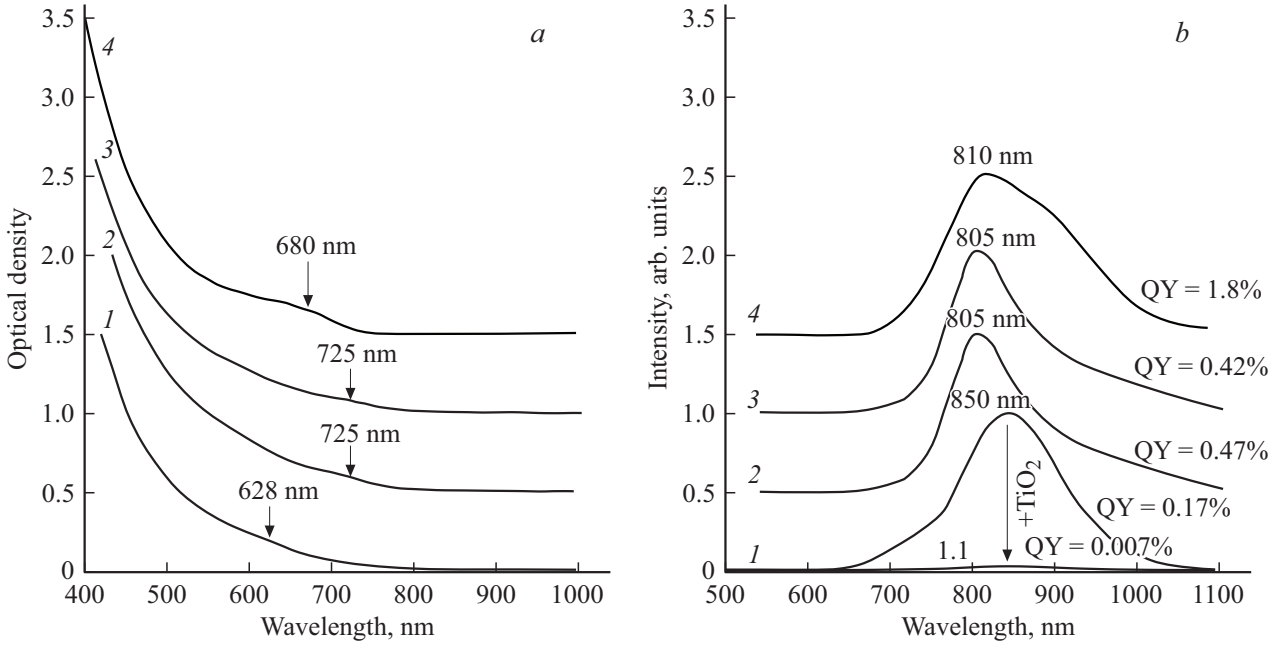

Figure 4. Absorption (a) and luminescence spectra (b) of samples: Ag_2S/2MPA/W — *1*, TiO_2-Ag_2S/2MPA/W — 1.1, Ag_2S/MPTMS — *2*, Ag_2S/SiO_2 — *3*, Ag_2S/2MPA/EG — *4*.

this is caused by behavior of ethylene glycol matrix forming micelles with QDs inside, as observed in TEM-images. Such micelles impede contact of QDs with the surface of TiO_2 nanoparticles and adsorption on their surface.

5. Absorption properties of the studied samples

In the optical absorption spectra of the studied samples of QDs there is size effect observed. Wide bands of optical absorption specific for semiconductor QDs are shifted into short-wave region relative to the edge of fundamendal absorption of Ag_2S monocrystals (1.0 eV [38]) and have the feature associated with the most probable exciton transition in the optical absorption (Fig. 4, *a*). Weak manifestation of that feature is most likely caused by heterogeneous broadening associated with QDs dispersion by size within the ensemble.

By using the data of main exciton transition position, the size of nanocrystals was estimated by using the Kayanuma Y. equation [39]. It turned out that the values of QDs average sizes lie in the range of 2.1−2.2 nm.

For the samples of Ag_2S/2MPA/W and Ag_2S/2MPA/EG QDs (Fig. 4, *a* the curves *1, 4*) feature in optical absorbtion spectra corresponding to the most probable exciton transition are located at 628 and 680 nm accordingly. The results of estimations of average sizes by using the Kayanuma Y. equation were close to the data obtained by using TEM (2.2 and 2.4 nm). For the samples of Ag_2S/MPTMS and Ag_2S/SiO_2 QDs (Fig. 4, *a* the curves *2* and *3*) there there is a red shift of feature in optical absorption spectra to the region to 725 nm, which is caused by growing of the crystalline nucleus Ag_2S due to the use of sulfur-containing precursor MPTMS. Such assumption is confirmed by the data of TEM and XRD.

The most important property of Ag_2S QDs in terms of photocatalysis is the possibility of their photoexcitation within a wide range from 750 to 400 nm, which is required for spectral sensitization of anatase nanocrystals.

Fig. 5 shows spectra of optical absorption of TiO_2 nanoparticles, pure, and decorated with various samples of Ag_2S QDs, obtained by the method of diffusion reflectance. The measured spectra of diffusion reflectance were built as Kubelka–Munk function:

$$F(R) = \frac{(1-R)^2}{2R}, \qquad (1)$$

where R — diffusion reflectance.

Approximation of the linear part of function enabled determination of the edge of fundamental absorption of the studied samples of TiO_2, which was about 3.2 eV, which corresponds to the bandgap width of crystalline anatase phase [40,41]. According to the obtained spectra it can be seen that TiO_2 (Fig. 4 the curve *1*) has absorption from 390 nm, which correlates with the data on the bandgap width of anatase (3.2 eV [40,41]). Samples of nanoparticles TiO_2, decorated with Ag_2S QDs, have considerable absorption within the visible region.

6. Luminescent properties of the samples

Fig. 4, *b* shows luminescence spectra of the studied samples in case of excitation by radiation with the wavelength

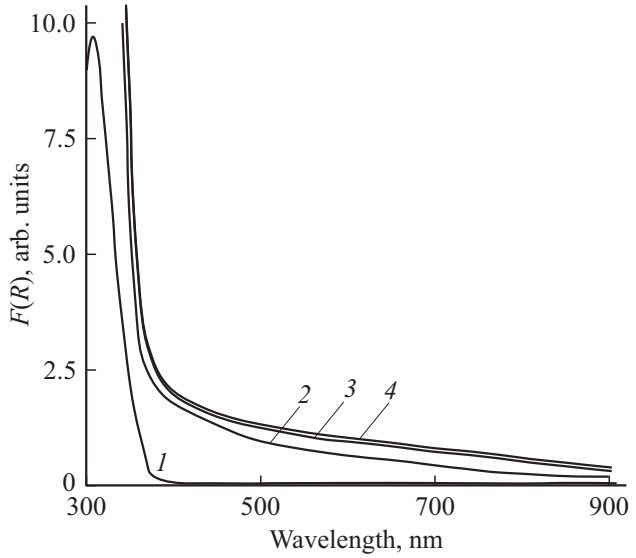

Figure 5. Spectra of optical absorption obtained by using the methodology of diffusion reflectance and Kubelka–Munk equation for the studied samples nanoparticles TiO_2 — *1*; nanoparticles TiO_2 decorated with QDs samples: Ag_2S/2MPA — *2*, Ag_2S/MPTMS — *3*, Ag_2S/SiO_2 — *4*.

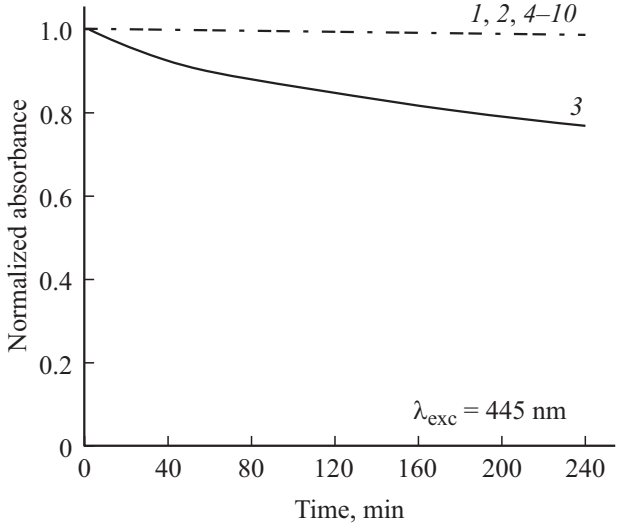

Figure 6. Dependence of normalized absorption within the band of methylene blue 665 nm on the time of exposure of the studied samples: MB^+ — *1*, $MB^+ + TiO_2$ — *2*, $MB^+ + TiO_2$-Ag_2S/2MPA/W — *3*, $MB^+ + TiO_2$-Ag_2S/MPTMS — *4*, $MB^+ + TiO_2$-Ag_2S/SiO_2 — *5*, $MB^+ + TiO_2$-Ag_2S/2MPA/EG — *6*, $MB^+ + Ag_2S$/2MPA/W — *7*, $MB^+ + Ag_2S$/MPTMS — *8*, $MB^+ + Ag_2S/SiO_2$ — *9*, $MB^+ + Ag_2S$/2MPA/EG — *10*.

of 445 nm. Ag_2S/2MPA/W QDs (Fig. 4, *b* the curve *1*) demonstrate luminescence in the near IR-region with the maximum in the region of 850 nm and quantum yield of 0.17%. The large full width at half maximum (FWHM) of the luminescence band and considerable Stokes shift relative to exciton transition in absorption, indicate luminescence occurring as a result of recombination of free hole with localized electron [24].

Replacement of solvent with ethylene glycol in case of Ag_2S/2MPA/EG QDs (Fig. 4, *b*, the curve *4*) results in shift of the maximum of luminescent band to 810 nm and increase of its quantum yield to 1.8%. The observed changes are caused by the interface nature of the centers of luminescence, which was discussed in publications many times [24–26,31].

Formation of shells results in 2.8 times increase of the quantum output of QDs luminescence up to 0.42 and 0.47%, accordingly. There is also short-wave shift of the maximum of luminescence by 45 nm with decrease of the Stokes shift relative to exciton transition in the absorption from 222 to 100 nm. Change in spectrum of luminescence is caused by formation of SiO_2 shell and change of interfaces of Ag_2S [42] QDs, as well as by limitation of penetration of the charge carriers into environment. The observed dependences turned out to be similar to the case when formation of Ag_2S/SiO_2 QDs takes place in ethylene glycol [30].

Decoration of TiO_2 nanoparticles with Ag_2S QDs resulted in changes in the luminescence spectrum only in case of the sample Ag_2S/2MPA/W QDs (Fig. 4, *b*, the curves *1* and *1.1*). For this sample the 25 times decrease in the luminescence quantum yield from 0.17 to 0.007% were observed. Taking into account the data of TEM, which demonstrate agglomeration of QDs near to the surface of Titanium Dioxide nanoparticles, the conclusion about possible charge carriers phototransfer were made. For other samples intensity and spectra of luminescence had not changed. In each of three cases QDs featured the shell of SiO_2, or viscous ethylene glycol. Therefore, regardless of the best luminescent properties of Ag_2S/2MPA/EG QDs, the indications of charge carriers phototransfer and formation of TiO_2-Ag_2S QDs is specific only for the case of decoration with Ag_2S/2MPA/W QDs.

Such conclusion is confirmed by the results of analysis of photobleaching of the methylene blue dye [43–45] in presence of the studied heterosystems (Fig. 6). Changes of optical density of methylene blue monomer absorption band (650−660 nm) were controlled during exctitation of heterosystem TiO_2-Ag_2S QDs with 445 nm radiation, which is beyond the region of TiO_2 absorption. Bleaching of methylene blue was observed only in the sample TiO_2-Ag_2S/2MPA/W (Fig. 6, the curve *3*). For all other samples, including separate components of heterosystem, there were no changes of optical density of methylene blue.

7. Conclusion

In this work, the analysis of structural and optical properties of colloidal Ag_2S QDs synthesized in various environment (Ag_2S/2MPA, Ag_2S/MPTMS, Ag_2S/SiO_2 in water, Ag_2S/2MPA in ethylene glycol) was made. The dependence of luminescence quantum yield of Ag_2S QDs on their interface state was studied. Increase of the

luminescence quantum yield of Ag_2S QDs up to 2.8 times (from 0.17 to 0.47%) as a result of SiO_2 shell formation was obseved. Impact of QDs environment on the possibility of charge carriers transfer between the components if TiO_2-Ag_2S QDs heterosystem was demonstrated and possibility of TiO_2-Ag_2S QDs heterostructure formation was analysed. As a result of analysis it was determined that the observed reduction of luminescence quantum yield from 0.17 to 0.007% at decoration of TiO_2 nanoparticles with Ag_2S/2MPA/W QDs is an indication of the charge phototransfer between the components of heterosystem. In other cases (Ag_2S/MPTMS, Ag_2S/SiO_2 in water, Ag_2S/2MPA in ethylene glycol) no such spectral manifestations were found. Formation of heterosystems TiO_2-Ag_2S enables producing the reactive oxygen species during excitation with visible range radiation, which was demonstrated by the photobleaching of methylene blue in presence of TiO_2 nanoparticles, decorated with Ag_2S/2MPA/W QDs. Use of mixtures of TiO_2 nanoparticles with water solutions of Ag_2S/MPTMS and Ag_2S/SiO_2 QDs, as well as Ag_2S/2MPA QDs in ethylene glycol did not provide sensitization of TiO_2 nanoparticles at that spectral range. Based on the obtained data we concluded that the possibility of formation of heterosystems TiO_2-Ag_2S, able of producing reactive oxygen species during excitation with visible range radiation, is highly dependent on the Ag_2S QDssurrounding, which ensures proper passivation of its interfaces and not impedes the charge transfer between the components of heterosystem.

Work funding

The work was carried out with support granted from the Russian Foundation for Fundamental Research No. 20-32-90167 Postgraduates. Structural studies performed by using the diffractometer THERMO ARL X'TRA (ThermoFisher, Switzerland) and transmission electron microscope LIBRA 120 (CarlZeiss, Germany) were done by using the equipment of the Research Equipment Sharing Center of Voronezh State University.

Conflict of interest

The authors declare that they have no conflict of interest.

References

[1] H.L. Chou, B.-J. Hwang, C.-L. Sun. New and Future Developments in Catalysis. Elsevier (2013) P. 217. doi 10.1016/B978-0-444-53880-2.00014-4
[2] J.J. Ng, K.H. Leong, L.C. Sim, W.-D. Oh, C. Dai, P. Saravanan. Nanomaterials for Air Remediation. Elsevier (2020) P. 193. doi 10.1016/B978-0-12-818821-7.00010-5
[3] M. Sakar, R.M. Prakash, K. Shinde, G.R. Balakrishna. Int. J. Hydrogen Energy. **45**, *13*, 7691 (2020). doi 10.1016/j.ijhydene.2019.04.222
[4] A. Kubackaa, U. Caudillo-Flores, I. Barba-Nieto, M. Fernández-García. Appl. Catal. A **610**, *25*, 117966 (2021). doi 10.1016/j.apcata.2020.117966
[5] S. Shen, C. Kronawitter, G. Kiriakidis. J. Materiomics **3**, *1*, 1 (2017). doi 10.1016/j.jmat.2016.12.004
[6] M. Pawar, S.T. Sendoğdular, P. Gouma. J. Nanomaterials **2018**, 5953609 (2018). doi 10.1155/2018/5953609
[7] A.L. Linsebigler, G. Lund, J.T. Yates Jr. Chem. Rev. **95**, *3*, 735 (1995). doi 10.1021/cr00035a013
[8] K. Nakata, A. Fujishima. J. Photochem. Photobiol. C **13**, *3*, 169 (2012). doi 10.1016/j.jphotochemrev.2012.06.001.
[9] J. Schneider, M. Matsuoka, M. Takeuchi, J. Zhang, Y. Horiuchi, M. Anpo, D.W. Bahnemann. Chem. Rev. **114**, *19*, 9919 (2014). doi 10.1021/cr5001892
[10] Z. Bao, S. Wang, X. Yu, Y. Gao, Z. Wen. Water Air Soil Pollut. **230**, 169 (2019). doi 10.1007/s11270-019-4219-5
[11] O.R. Fonseca-Cervantes, A. Perez-Larios, V.H. Romero Arellano, B. Sulbaran-Rangel, C.A. Guzman Gonzalez. Processes **8**, *9*, 1032. (2020). doi 10.3390/pr8091032.
[12] M. Janczarek, E. Kowalska. Catalysts **7**, *11*, 317 (2017). doi 10.3390/catal7110317
[13] S.B. Rawal, S. Bera, D. Lee, D.-J. Jang, W. In Lee. Catal. Sci. Technol., **3**, 1822 (2013). doi 10.1039/C3CY00004D
[14] C. Del Cacho, O. Geiss, P. Leva, S. Tirendi, J. Barrero-Moreno. Nanotechnology in Eco-Efficient Construction. Woodhead Publishing (2013) P. 343. doi 10.1533/9780857098832.3.343
[15] I. Zumeta-Dube, V.-F. Ruiz-Ruiz, D. Diaz, S. Rodil-Posadas, A. Zeinert. Phys. Chem. C, **118**, *22*, 11495 (2014). doi 10.1021/jp411516a
[16] A. Badawi. Physica E **109**, 107 (2019). doi 10.1016/j.physe.2019.01.018.
[17] R. Gui, H. Jin, Z. Wang, L. Tan, Coord. Chem. Rev. **296**, *15*, 91 (2015). doi 10.1016/j.ccr.2015.03.023
[18] R. Gui, A. Wan, X. Liu, W. Yuan, H. Jin. Nanoscale **6**, *10*, 5467 (2014). doi 10.1039/C4NR00282B
[19] R. Gui, J. Sun, D. Liu, Y. Wang, H. Jin. Dalton Trans. **43**, *44*, 16690 (2014). doi 10.1039/C4DT00699B
[20] R. Tang, J. Xue, B. Xu, D. Shen, G.P. Sudlow, S. Achilefu. ACS Nano **9**, *1*, 220 (2015). doi 10.1021/nn5071183
[21] Y. Xie, S.H. Yoo, C. Chen, S. Oh. Mater. Sci. Eng. B **177**, *1*, 106. (2012). doi 10.1016/j.mseb.2011.09.021
[22] B. Liu, D. Wang, Y. Zhang, H. Fan, Y. Lin, T. Jiang, T. Xie. Dalton Trans. **42**, 2232 (2014). doi 10.1039/C2DT32031B
[23] K. Nagasuna, T. Akita, M. Fujishima, H. Tada. Langmuir. **27**, *11*, 7294 (2011). doi 10.1021/la200587s
[24] M. Smirnov, O. Ovchinnikov. J. Lumin. **227**, 117526 (2020). doi 10.1016/j.jlumin.2020.117526
[25] O.V. Ovchinnikov, I.G. Grevtseva, M.S. Smirnov, T.S. Kondratenko, A.S. Perepelitsa, S.V. Aslanov, V.U. Khokhlov, E.P. Tatyanina, A.S. Matsukovich. Opt. Quantum Electron. **52**, *4*, 198 (2020). doi 10.1007/s11082-020-02314-8
[26] O.V. Ovchinnikov, M.S. Smirnov, B.I. Shapiro, T.S. Shatskikh, A.S. Perepelitsa, N.V. Korolev. Semiconductors **49**, *3*, 373 (2015). https://doi.org/10.1134/S1063782615030173
[27] C.M. Wilke, C. Petersen, M.A. Alsina, J.-F. Gaillard, K.A. Gray. Environ. Sci.: Nano, **6**, 115 (2019). doi 10.1039/C8EN01159A
[28] X. Liu, L. Zhu, X. Wang, X. Meng. Env. Sci. Pollution Res., **27**, 13590 (2020). doi 10.1007/s11356-020-07960-9
[29] T.S. Kondratenko, M.S. Smirnov, O.V. Ovchinnikov, A.I. Zvyagin, T.A. Chevychelova, I.V. Taydakov. Bull. Lebedev Phys. Inst. **46**, 210 (2019). doi /10.3103/S106833561906006X

[30] O.V. Ovchinnikov, S.V. Aslanov, M.S. Smirnov, A.S. Perepelitsa, T.S. Kondratenko, A.S. Selyukov, I.G. Grevtseva. Opt. Mater. Express **11**, *1*, 89 (2021). doi 10.1364/OME.411432
[31] O.V. Ovchinnikov, S.V. Aslanov, M.S. Smirnov, I.G. Grevtseva, A.S. Perepelitsa. RSC Adv. **9**, 37312 (2019). doi 10.1039/C9RA07047H
[32] J.R. Lakowicz. Principles of Fluorescence Spectroscopy. Springer, N.Y. (2006). doi 10.1007/978-0-387-46312-4
[33] S. Reindl, A. Penzkofer, S.-H. Gong, M. Landthaler, R.M. Szeimies, C. Abels, W. Baumler. J. Photochem. Photobiol. A **105**, 65 (1997). doi 10.1016/S1010-6030(96)04584-4
[34] A.J. Frueh. Z. Kristallogr. **110**, 136 (1958).
[35] H.F. Poulsen, J. Neuefeind, H.-B. Neumann, J.R. Schneider. J. Non-Crystalline Solids **188**, *1*, 74 (1995). doi 10.1016/0022-3093(95)00095-X
[36] S. Music, N. Filipovic-Vincekovic, L. Sekovanic. Braz. J. Chem. Eng. **28**, *1*, 89 (2011). doi 10.1590/S0104-66322011000100011
[37] H. Ijadpanah-Saravy, M. Safari, A. Khodadadi-Darban, A. Rezaei. Anal.Lett. **47**, *10*, 1772 (2014). doi: 10.1080/00032719.2014.880170
[38] S. Lin, Y. Feng, X. Wen, P. Zhang, S. Woo, S. Shrestha, G. Conibeer, S. Huang. J. Phys. Chem. **119**, 867 (2015). doi 10.1021/jp511054g
[39] Y. Kayanuma. Phys. Rev. B: Condens. Matter Mater. Phys. **38**, 9797 (1988). doi 10.1103/PhysRevB.38.9797
[40] A.B. Murphy. Solar Energy Mater. Solar Cells **91**, *14*, 1326 (2007). doi 10.1016/j.solmat.2007.05.005
[41] V.M. Ievlev, S.B. Kushchev, A.N. Latyshev, L.Yu. Leonova, O.V. Ovchinnikov, M.S. Smirnov, E.V. Popova, A.V. Kostyuchenko, S.A. Soldatenko. FTP (in Russian) **48**, *7*, 875 (2014).
[42] A.S. Perepelitsa, O.V. Ovchinnikov, M.S. Smirnov, T.S. Kondratenko, I.G. Grevtseva, S.V. Aslanov, V.Y. Khokhlov. J. Luminescence **231**, 117805 (2021). doi 10.1016/j.jlumin.2020.117805
[43] A. Mills, J. Wang. J. Photochem. Photobiol. A **124**, *1*, 123 (1999) doi 10.1016/S1010-6030(99)00143-4
[44] S. Otsuka-Yao-Matsuo, T. Omata, S. Ueno, M. Kita. Mater. Transact. **44**, *10*, 2124 (2003).
[45] J. Yao, C. Wang. Int. Photoenergy **2010**, 643182 (2010). doi:10.1155/2010/643182